*Clays and Clay Minerals*, Vol. 43, No. 6, 656–668, 1995.

# INFLUENCE OF NONSTOICHIOMETRY AND THE PRESENCE OF MAGHEMITE ON THE MÖSSBAUER SPECTRUM OF MAGNETITE†

G. M. DA COSTA,[1,2] E. DE GRAVE,‡,[1] P. M. A. DE BAKKER,[1] and R. E. VANDENBERGHE[1]

[1] Laboratory of Magnetism, Department of Subatomic and Radiation Physics, University of Gent, B-9000 Gent, Belgium

[2] On leave from Departamento de Química, Universidade Federal de Ouro Preto, Ouro Preto, MG, Brazil

**Abstract**—Several samples of large- and small-particle magnetite ($Fe_3O_4$), as well as its thermal decomposition products formed at different temperatures and atmospheres, have been studied extensively by Mössbauer spectroscopy (MS), both with and without an applied field of 6T. Synthetic mixtures of magnetite and poorly- or well-crystallized maghemite have also been studied. Large-particle magnetite (MCD > 200 nm), when heated in air for 12 hours at T < 400°C, transforms to a mixture of well-crystallized hematite and magnetite, the latter one remaining stoichiometric, according to the relative area-ratios obtained from MS. Thermal treatment at 1300°C in a controlled $O_2$ partial pressure, produced a mixture of stoichiometric and nonstoichiometric magnetite, but the latter component seems to be composed of particles with different degrees of nonstoichiometry. The Mössbauer spectra of the decomposition products at T < 200°C in air of small-particle magnetite (MCD ~ 80 nm) could be successfully interpreted as a mixture of magnetite and maghemite, rather than nonstoichiometric magnetite. This suggestion is further supported by the experiments with the synthetic mixtures. It is clearly demonstrated that is not possible, even by applying a strong external field, to separate the contribution of the A-site of magnetite from that of maghemite.

**Key Words**—Magnetite, Mössbauer effect, Nonstoichiometric magnetite.

## INTRODUCTION

Since the discovery of the Mössbauer effect in iron, a huge number of papers dealing with that effect in magnetite ($Fe_3O_4$) and maghemite ($\gamma$-$Fe_2O_3$) have been published (Vandenberghe and De Grave 1989 and references therein). In spite of that, some features of these oxides' Mössbauer spectra remain puzzling. One question that intrigues many Mössbauer spectroscopists with interests in soil-related oxides is whether or not one can distinguish, by Mössbauer spectroscopy, between nonstoichiometric magnetite on the one hand, and a mixture of magnetite and maghemite on the other hand.

Both magnetite and maghemite have a spinel structure in which the cations occupy tetrahedral (A) and octahedral (B) interstices. Magnetite is usually represented by the formula $Fe^{3+}[Fe^{2+}Fe^{3+}]O_4$, with the cations between brackets representing the ones in octahedral sites. Its Mössbauer spectrum (MS) at room temperature (RT) is commonly interpreted as a superposition of two patterns, one due to trivalent iron on A sites, and the other to $Fe^{2.5+}$ on B sites. Separate patterns for $Fe^{2+}$ and $Fe^{3+}$ on B sites are not observed due to a fast electron exchange between these cations. The nature of this exchange process has been interpreted either as a pair-wise hopping process or as a global delocalization of the sixth 3d electron of the $Fe^{2+}$ ions into a conduction band involving the entire octahedral sublattice (Vandenberghe and De Grave 1989). The two models seem to be complimentary, and neither of the two is able to explain the whole of observed magnetic and electronic properties of magnetite. The inclusion of a certain concentration of impurities on B sites, be it vacancies and/or substitutional cations other than iron, seems to favor a more localized electron-exchange process (Vandenberghe and De Grave 1989; De Grave *et al* 1993). Typical values for the hyperfine parameters of well-crystallized magnetite at room temperature are (Daniels and Rosencwaig 1969): $H_{hf,A}$ = 490 kOe, $\delta_A$ = 0.29 mm/s, $H_{hf,B}$ = 460 kOe, $\delta_B$ = 0.66 mm/s and $\epsilon_Q$ = 0 for both sites, where $H_{hf}$ is the hyperfine field, $\epsilon_Q$ the quadrupole shift and $\delta$ the center shift quoted relative to metallic iron. Recording the spectrum in the presence of a strong external magnetic field results in a better separation of the two sextets since the external-field value adds to the A-site and subtracts from the B-site hyperfine field. Thus, for a typical external field of 60 kOe one should have $H_{eff,A} \cong 550$ kOe and $H_{eff,B} \cong 400$ kOe, where $H_{eff}$ is the effective field, i.e., the magnitude of the vectorial sum of hyperfine and applied field. The relative area ratio of the two spectral components at RT is close to 1:1.88; it is not exactly 1:2, as would be expected by considering the chemical formula, due to different recoilless fractions (Sawatzky *et al* 1969). For completeness, it

† Contribution #SSF95-01-08 from the Department of Subatomic and Radiation Physics, University of Gent.

‡ Research Director, National Fund for Scientific Research, Belgium.

should be mentioned that several authors (Häggström *et al* 1978, De Grave *et al* 1993) considered two B-site patterns at RT, with a relative abundance 1:3. The explanation for that interpretation is that the magnetite moments are aligned along a domain's [100] axis, while the electric field gradient (EFG) has its principal axis along a local [111] direction, resulting in two distinct quadrupole shifts and dipolar-field contributions to $H_{hf,B}$.

Maghemite differs from magnetite in that it contains no divalent iron species. It can be represented by the formula $Fe^{3+}[Fe^{3+}_{5/3}\square_{1/3}]O_4$, where again the brackets represent octahedral sites. The vacancies (□) are also reported to occur in both sites simultaneously (Armstrong *et al* 1966; Annersten and Hafner 1977; Haneda and Morrish 1977). The zero-field room temperature Mössbauer spectrum is composed of two sextets, but their hyperfine parameters are so close to one another that they can only be distinguished by numerical deconvolution. It has recently been shown that the A-site center shift is approximately 0.12 mm/s less than $\delta_B$, at any temperature (da Costa *et al* 1994a). The hyperfine parameters for a relatively well-crystallized sample at 275K, as determined from measurements in an external field of 60 kOe, are:

$$H_{hf,A} = (506 \pm 4)\ \text{kOe},\ \delta_A = (0.233 \pm 0.005)\ \text{mm/s},$$
$$H_{hf,B} = (507 \pm 4)\ \text{kOe},$$

$\delta_B = (0.357 \pm 0.005)$ mm/s and $\epsilon_Q = 0$ for both sites (da Costa *et al* 1994a). Line broadening, especially for poorly crystalline members, has frequently been observed and is unanimously attributed to distributions on the hyperfine fields. A diversity of phenomena have been suggested in order to explain the origin of these field distributions, including collective magnetic excitations (Mørup *et al* 1976), surface effects (de Bakker *et al* 1991), and inter-particle magnetic interactions (Mørup and Tronc 1994).

Nonstoichiometric magnetite can be represented by the formula $Fe_{3-v}O_4$, where v can, in principle, range from zero (pure magnetite) to 0.333 (maghemite). If one considers that hopping occurs only between pairs of ferrous and ferric irons, it can also be represented by the formula:

$$Fe^{3+}[Fe^{2+}_{1-y}\ Fe^{3+}_{1-y}Fe^{3+}_{5y/3}\square_{y/3}]O_4 \qquad y = 3v$$

The hyperfine fields for $Fe^{3+}$ in tetrahedral sites ($Fe^{3+}_A$) and for $Fe^{2.5+}$ in octahedral sites ($Fe^{2.5+}_B$) should not be too much different from those in stoichiometric magnetite. On the other hand, the unpaired $Fe^{3+}$ in octahedral sites ($Fe^{3+}_B$) are expected to have a hyperfine field close to 500 kOe and $\delta = 0.39$ mm/s, as observed in maghemite (Coey *et al* 1971). Actually, the zero-field spectrum at RT of nonstoichiometric magnetite closely resembles that of pure magnetite, but the area ratio of the two sub-patterns deviates from 1:1.88 because there are less ferrous ions and the unpaired octahedral ferric ions contribute to the apparent A-site absorption.

Magnetite undergoes a phase transition near $T_V$ = 120 K, known as the Verwey transition (Verwey and Haayman 1941). The Mössbauer spectrum below $T_V$ is quite different from that at higher temperatures, and considerable controversy still exists regarding its interpretation. It has been found that for homogeneous single crystals of nonstoichiometric magnetite, the transition temperature decreases continuously with the degree of nonstoichiometry (Aragon *et al* 1985; Kakol and Honig 1989). The shape of the Mössbauer spectrum near $T_V$ changes dramatically within a few degrees for pure $Fe_3O_4$ ($T_V$ = 121 K), whereas for highly nonstoichiometric samples (v = 0.03) this transition is spread-out over a much broader interval (Haley *et al* 1989). Hence, by measuring $T_V$ with the aid of MS, one should in principle be able to determine the degree of nonstoichiometry in a particular sample (Steinthorsson *et al* 1992). The main problem for this approach is that other effects such as dislocations and strains also lower $T_V$ to a value as low as 104 K, as shown by Iida (1980) for a single-crystal specimen. Thus, it seems that the observation of a lower $T_V$ for a given magnetite sample is not a conclusive proof for the existence of a nonstoichiometric composition. Furthermore, all the above quoted results with respect to the effect of nonstoichiometry upon $T_V$ were obtained for single crystals, and the behavior of small-particle systems is most likely different. In that respect, it is worth mentioning that samples which seem to be really nonstoichiometric have all been prepared at very high temperatures and under controlled partial pressure of oxygen (Coey *et al* 1971; Dieckmann and Schmalzried 1977; Aragon *et al* 1985; Randani *et al* 1987).

Chemical analyses have commonly been used to determine the amount of $Fe^{2+}$ in nonstoichiometric magnetites, but the agreement between their results and those derived from the MS was usually very poor (Randani *et al* 1987). It is well known that the determination of ferrous ions is extremely susceptible to errors due to oxidation during the dissolution procedure, especially for large particles which are more resistant to the acid attack. So, unless the analysis is carried out meticulously, the reported results should be considered with caution.

Another important question concerns the stability range of nonstoichiometric magnetite. Using thermogravimetric titration, Dieckmann (1982) showed that the maximum value for v is 0.01 at 900°C and 0.09 at 1400°C. Values for v higher than 0.20 have been reported for small-particle samples (MCD < 100 nm) prepared by heating magnetite under air at low temperatures (Annersten and Hafner 1973; Murad and Schwertmann 1993). It is clear from these findings that results obtained from single crystals cannot be compared with those of small-particle systems.

In this paper the authors present a careful Mössbauer and X-ray diffraction (XRD) analysis of synthetic samples of maghemite, magnetite and nonstoichiometric magnetite. The main objective is to determine if a mixture maghemite-magnetite can be distinguished, by Mössbauer spectroscopy, from nonstoichiometric magnetite. This question is of significant importance in connection to the characterization of magnetic soils by means of Mössbauer spectroscopy.

## EXPERIMENTAL

Powder XRD patterns were obtained using a Philips diffractometer with CoK$\alpha$ radiation and a graphite monochromator. The scans were done in the range of 15–80° (2$\theta$) at a speed of 1/4° min$^{-1}$, and the reflected intensities were recorded in a multichannel analyser. Some samples were also step-scanned from 89° to 92° (2$\theta$), with a step of 0.01° and a counting time of 40 seconds per channel. The latter measurements were performed on a Siemens D-5000 diffractometer equipped with Cu-tube and a graphite monochromator. The digital patterns were fitted with a sum of pseudo-Lorentzian peak-shape functions, two for each reflection in order to account for the superposition of K$\alpha$1 and K$\alpha$2 radiation. Mean crystallite diameters (MCD) were estimated from the full width at half maximum (FWHM) using Scherrer's equation with K = 0.9 (Klug and Alexander 1974). The instrumental contribution to the peak width was evaluated from the diffractogram of a well-crystallized commercial hematite sample, annealed at 1000°C in oxygen atmosphere for 24 hours in order to optimize the crystallinity. Lattice parameters were determined by the Nelson-Riley extrapolation method (Klug and Alexander 1974).

Mössbauer spectra were recorded using a time-mode spectrometer with a constant-acceleration drive and a triangular reference signal. All absorbers were prepared by mixing an amount of material with very pure carbon in order to achieve a homogeneous thickness of approximately 10 mg Fe/cm$^2$. The spectrometer was periodically calibrated using the spectrum of the same hematite described above. External field ($H_{ext}$) of 60 kOe parallel to the direction of the incident $\gamma$-rays was applied either at 275 K, or at 130 K. For these experiments the calibration spectra were recorded simultaneously using another source and counting electronics at the opposite end of the transducer. Center shifts are quoted relative to metallic iron.

## RESULTS AND DISCUSSION

### *Mössbauer results*

*Large-particle magnetite.* Sample MM0 is a commercial magnetite (Agfa) that has been stored for many years without any particular protection against oxidation. Its X-ray diffractogram shows that it contains a small amount of hematite as an impurity phase. Size estimation is not feasible because the line width is almost the same to that of the reference material used to calibrate the equipment, indicating that the particle size is larger than 200 nm.

The sample has been subjected to thermal treatment for 12 hours in air at 200°C (MM0C), 300°C (MM0D) and 400°C (MM0E). The MS at RT, (Figure 1) have been successfully interpreted as a superposition of three sextet components, with the highest $H_{hf}$ being due to hematite. Pure Lorentzian-shaped sextets were used with line-area ratios fixed at 3:2:1 and quadrupole shifts $\epsilon_Q = 0$ for both sites of magnetite. The hyperfine parameters for the hematite phase, when it occurs with less than 5% of the total absorption, were fixed at their values found for sample MM0E, which contains 28% of this component (see below).

As seen from Table 1, all calculated hyperfine parameters have remained unchanged by the thermal treatment. The only difference from one sample to another is the relative area of the hematite component, which rises with increasing temperature of treatment. Another important parameter derived from the spectra is the occupation number (N), i.e., the ratio of iron atoms in octahedral and tetrahedral sites of magnetite. As reported in Table 1, this ratio is close to 2.0, regardless of the amount of hematite present in the samples, meaning that the remaining magnetite keeps its initial, near-stoichiometric composition.

In general, the final products resulting from thermal treatment of magnetite are strongly dependent on the conditions used to perform the transformation. Thus, the temperature, atmosphere, heating time, particle size and the presence of water all seem to play an important role in that respect (Bate 1975). The present results are in agreement with those reported by Elder (1965), who has demonstrated that large-particle magnetite converts only into hematite when heated under air, regardless of the presence of water. Furthermore, we have shown that the non-converted magnetite remains stoichiometric, at least as far as the Mössbauer results are concerned.

Finally, the hematite hyperfine fields (see Table 1) are very close to the saturation value for bulk samples, for which $H_{hf}$ equals 517 kOe at room temperature. This fact, together with the stoichiometry of the remaining magnetite, suggest that once the reaction has been initiated in one particular grain it continues until completion within the boundaries of that grain, rather than forming a thin layer around the grain.

*Small-particle magnetite.* This sample, further denoted as MMA0, was prepared according to the procedure described by Sugimoto and Matijevic (1980). The following solutions were mixed in a three-port flask under

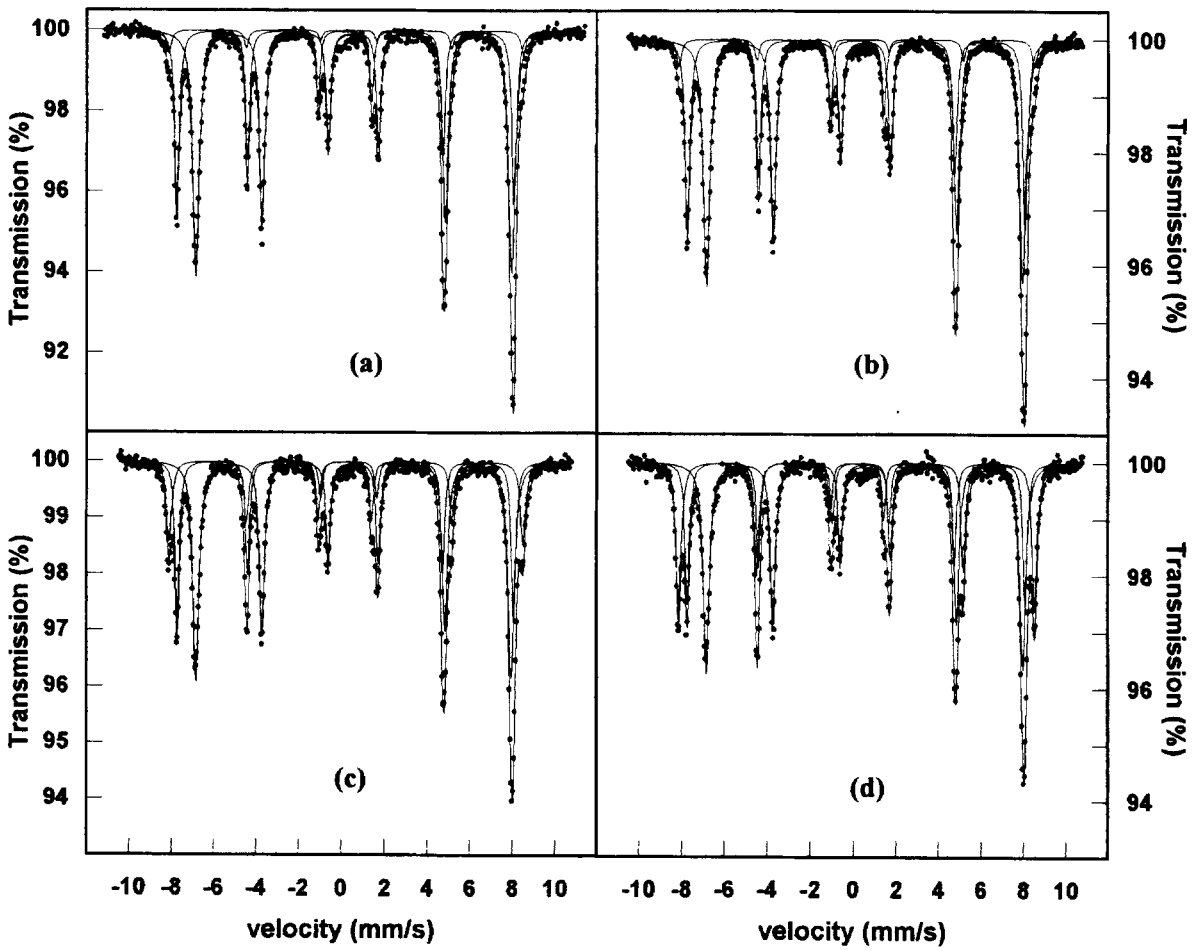


Figure 1. Room temperature Mössbauer spectra of large-particle magnetite: a) MM0, b) MM0 heated at 200°C, c) MM0 heated at 300°C, and d) MM0 heated at 400°C. The high-field absorption is due to hematite. Full lines represent the calculated spectra and their sum.

constant purging with nitrogen: 150 $cm^3$ of 0.5 M KOH, 30 $cm^3$ of 2.0 M $KNO_3$ and 30 $cm^3$ of 0.25 M $FeSO_4$. After dilution to 300 $cm^3$ with water, the system was kept at 90°C without agitation. After thirty minutes the black precipitate was centrifuged, washed several times with $O_2$-free water and then dried at 40°C under air. Bi-distilled water in which oxygen-free nitrogen was bubbled for two hours was used to prepare all solutions. The solid material was stored at room temperature under air. According to the XRD pattern, the MCD along the [311] direction is approximately 80 nm.

The room-temperature MS of the freshly prepared sample is shown in Figure 2a. This spectrum has been adjusted with two Lorentzian-shaped sextets using the following constraints: line-area ratios 3:x:1, quadrupole shift fixed at zero and independent widths for each

Table 1. Mössbauer parameters as derived from the room temperature spectra of samples MM0, MM0C, MM0D and MM0E. The full widths of lines 1 and 6 are given by $\Gamma_{1,6}$. N is the ratio of iron atoms in octahedral and tetrahedral sites of magnetite.

| | $Fe_3O_4$ | | | | | | | | | $\alpha$-$Fe_2O_3$ | | | |
|---|---|---|---|---|---|---|---|---|---|---|---|---|---|
| Sample | $H_{hf,A}$ (kOe) | $\delta_A$ (mm/s) | $\Gamma_{1,6}$ (mm/s) | RA (%) | $H_{hf,B}$ (kOe) | $\delta_A$ (mm/s) | $\Gamma_{1,6}$ (mm/s) | RA (%) | N | $H_{hf}$ (kOe) | $\delta$ (mm/s) | $\Gamma_{1,6}$ (mm/s) | RA (%) |
| MM0 | 491 | 0.265 | 0.25 | 33 | 459 | 0.662 | 0.35 | 63 | 2.0 | 517 | 0.367 | 0.29 | 4 |
| MM0C | 490 | 0.267 | 0.26 | 35 | 458 | 0.661 | 0.37 | 60 | 1.9 | 517 | 0.367 | 0.28 | 5 |
| MM0D | 490 | 0.264 | 0.26 | 28 | 459 | 0.659 | 0.35 | 55 | 2.1 | 515 | 0.366 | 0.30 | 17 |
| MM0E | 490 | 0.267 | 0.26 | 24 | 459 | 0.663 | 0.35 | 48 | 2.1 | 517 | 0.367 | 0.28 | 28 |

https://doi.org/10.1346/CCMN.1995.0430602 Published online by Cambridge University Press

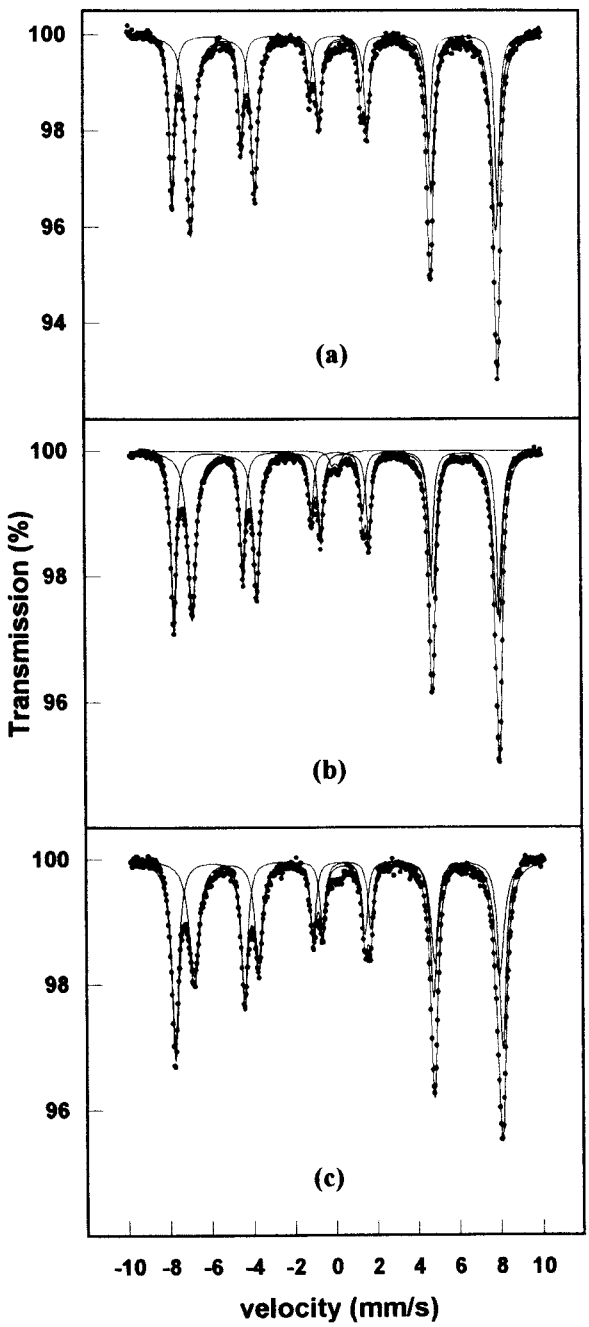


Figure 2. Room temperature Mössbauer spectra of small-particle magnetite: a) freshly prepared (MMA0), b) previous sample after one month exposed to air at room temperature (MMA0N), c) sample MMA0 heated at 80°C during 24 hours (MMA0H).

sextet. Typical iterated values for x ranged from 1.95 to 2.1. A small absorption near the center of the spectrum could not be fitted properly due to its low intensity (see below). The parameters derived from the fit are given in Table 2, and are in agreement with literature

Table 2. Mössbauer parameters at room temperature (upper part) and at 275 K under an applied field of 60 kOe (lower part) of some selected samples. Estimated errors are: 1 kOe for the effective fields ($H_{eff}$), 4 kOe for the hyperfine fields ($H_{hf}$) and 0.01 mm/s for the isomer shifts ($\delta$).

| | $Fe_3O_4$ | | | | | | | | | $\gamma$-$Fe_2O_3$ | | | | | |
|---|---|---|---|---|---|---|---|---|---|---|---|---|---|---|---|
| Sample | $H_{effA}$ (kOe) | $H_{hfA}$ (kOe) | $\delta_A$ (mm/s) | RA (%) | $H_{effB}$ (kOe) | $H_{hfB}$ (kOe) | $\delta_B$ (mm/s) | RA (%) | $H_{effB}$ (kOe) | $H_{hfB}$ (kOe) | $\delta_B$ (mm/s) | RA (%) | $H_{effA}$ (kOe) | $H_{hfA}$ (kOe) | $\delta_A$ (mm/s) | RA (%) |
| MMA0 | – | 488 | 0.27 | 34 | – | 458 | 0.66 | 66 | – | – | – | – | – | – | – | – |
| MMA0N | – | 489 | 0.27 | 40 | – | 458 | 0.65 | 58 | – | – | – | – | – | – | – | – |
| MMA0H | – | 491 | 0.28 | 53 | – | 458 | 0.65 | 45 | – | – | – | – | – | – | – | – |
| MMA0N* | 553 | 493 | 0.30 | 34 | 408 | 468 | 0.69 | 56 | 436 | 496 | 0.38 | 10 | – | – | – | – |
| MMA0H* | 554 | 494 | 0.30 | 33 | 407 | 467 | 0.68 | 43 | 447 | 507 | 0.40 | 24 | – | – | – | – |
| MMA0N | 554 | 494 | 0.30 | 30 | 408 | 468 | 0.69 | 56 | 437 | 497 | 0.37 | 9 | 547 | 487 | 0.25 | 5 |
| MMA0H | 557 | 497 | 0.30 | 23 | 407 | 467 | 0.68 | 43 | 448 | 508 | 0.41 | 21 | 551 | 491 | 0.29 | 13 |

* The last four numerical data do not correspond to the B-site of maghemite.

https://doi.org/10.1346/CCMN.1995.0430602 Published online by Cambridge University Press

values for stoichiometric magnetite, especially as far as the relative areas are concerned.

Figure 2b shows the spectrum of sample MMA0 one month after synthesis (sample MMA0N). It is evident that the area ratio has decreased, as can be seen from the Mössbauer parameters given in Table 2. The value for N has dropped to approximately 1.5, indicating that this sample could be a nonstoichiometric magnetite. The absorption in the central part of the spectrum is now sufficiently intense to be fitted, and a doublet with a quadrupole splitting ($\Delta E_Q$) of 0.34 mm/s and $\delta = 0.092$ mm/s has been successfully adjusted. A fixed line width of 0.35 mm/s had to be imposed. This doublet accounts for 1.6% of the total absorption and its origin could not be established.

Thermal treatment of sample MMA0 at several temperatures, usually less than 200°C, has produced materials for which N varies with the heating time and/or temperature. A typical example is sample MMA0H, which was obtained after heating at 80°C for 24 hours in air. Its MS is shown in Figure 2c, and the parameters obtained from a two-sextet fit are listed in Table 2. The occupation number for this sample is 0.9. The A-site hyperfine field is 2 kOe higher than for MMA0, whereas it has remained unchanged for the octahedral site. Although this increase is rather small, it is believed to be significant since it has been observed by Murad and Schwertmann (1993) in magnetites of similar crystallinity. A possible explanation for this higher hyperfine field is given in the text below.

As explained in the Introduction, a strong external field should enable to separate any absorption due to $Fe^{3+}$ in octahedral sites from that due to $Fe^{3+}$ in tetrahedral ones, the sample being either nonstoichiometric magnetite or a mixture maghemite-magnetite. Figure 3 shows the 60 kOe applied-field spectra of samples MMA0N and MMA0H. For both a third component is evident, which is less intense for sample MMA0N. It should be stressed at this point that the $\Delta m_I = 0$ transitions (middle lines at velocities in the vicinity of $-3$ and $+4$ mm/s) have not completely vanished, in contrast to what is observed for stoichiometric magnetite (De Grave *et al* 1993). These middle lines most probably can be attributed to the presence of a minor fraction of small-particle maghemite.

At first glance a three-sextets fit would be adequate to describe the applied-field data (Figures 3a and 3b). For this first attempt the same restrictions to those imposed in fitting the MMA0 spectra at RT were used, and the relevant parameters are given in Table 2. A surprising result concerns the values found for the $Fe_A^{3+}$ and $Fe_B^{2.5+}$ hyperfine fields. These values are expected to be the same as those determined from the zero-field spectra. This is indeed observed to be the case for $Fe_A^{3+}$, but not so for $Fe_B^{2.5+}$ for which a difference of about 10 kOe is obtained. A similar phenomenon has recently been pointed out and discussed by De Grave *et al* (1993) for magnetites containing up to 0.04 Co cations per formula unit, and the reader is referred to that paper for further details. It is further important to realize that the center shift for the $Fe_B^{3+}$ component is very close to the value for isolated ferric ions, as found for example in maghemite (da Costa *et al* 1994a). This means that the corresponding ferric ions, if present in the magnetite lattice, do not participate in the hopping process. This suggests a pair-localized character for the electron-exchange process. This suggestion is in agreement with the results and their interpretation as reported by Daniels and Rosencwaig (1969).

At this point, it seems pertinent to check all the results presented above with respect to the chemical formula indicated in the Introduction for nonstoichiometric magnetite. From this formula, two relations between the unknown degree of nonstoichiometry y and experimentally observable area ratios can be derived:

$$\frac{Fe_B^{2.5+}}{Fe_A^{3+}} = 2 - 2y$$

and

$$\frac{Fe_B^{3+}}{Fe_A^{3+}} = 1.666y$$

Using the relative areas as obtained from the in-field spectra (Table 2) for sample MMA0H and a value of 0.94 for $f_B/f_A$ for magnetite (Sawatzky *et al* 1969), and assuming equal recoilless-fraction for ferric ions regardless of their coordination, the first equation yields $y = 0.31 \pm 0.04$, and in the second equation $y = 0.44 \pm 0.06$. The errors in y were calculated by considering a reasonable inaccuracy of 10% for the experimental values of the relative areas. The difference between these two y values, even taking into account the errors, is rather large. Possible explanations for this discrepancy are that the proposed formula is not correct, or that vacancies could have entered both lattice sites. It is easily calculated that for this latter case the composition which would be consistent with the observed area ratios can be written as:

$$(Fe^{3+}_{0.93}\square_{0.07})[Fe^{2+}_{0.65}Fe^{3+}_{0.65}Fe^{3+}_{0.66}\square_{0.04}]O_4$$

This high vacancy concentration in tetrahedral sites is unlikely to be realistic.

A third possible cause for the inconsistent y data is that the involved sample is a mixture of magnetite and maghemite, rather than a single-phase, nonstoichiometric magnetite. If a few additional, but nevertheless reasonable parameter restrictions are imposed in the fitting procedure, a sum of four sextets is readily adjusted to the experimental data, as shown in Figures 3c and 3d. These constraints were: fixed A- to B-area ratio of 1:1.88 for the magnetite component, and 0.375:0.625 for maghemite component, and additionally $\delta_A$

https://doi.org/10.1346/CCMN.1995.0430602 Published online by Cambridge University Press

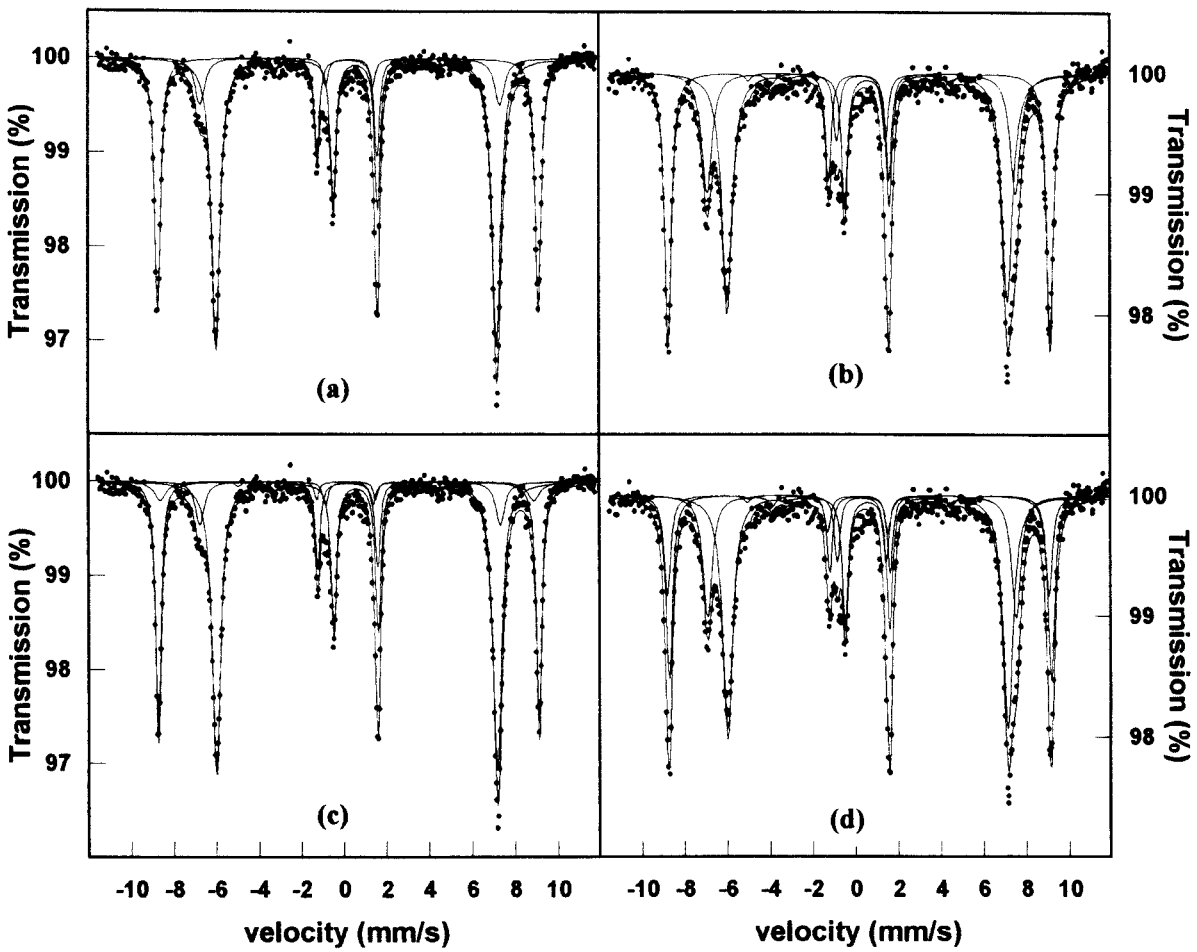


Figure 3. Applied-field (6 Tesla) Mössbauer spectra at 275 K of small-particle magnetite. Spectra fitted with three sextets: a) MMA0 and b) MMA0H. Figures 3c and 3d depict a four-sextets fit to the same spectra.

$= \delta_B - 0.12$ mm/s for the latter one. Different line widths were used for each sextet. In this way the parameters listed in Table 2 were obtained, which are all within the range of acceptable values for both magnetite and maghemite. Thus, sample MMA0H could be a mixture of approximately 30% of maghemite and 70% of magnetite. Of course, more complicated mixtures of magnetite/maghemite and nonstoichiometric magnetites, with different amounts of each component and/or degrees of nonstoichiometry, could be proposed to comply with the Mössbauer results. In conclusion, as far as Mössbauer spectroscopy is concerned, it seems to be impossible to correctly define the composition of sample MMA0H and related samples.

*Synthetic mixtures of magnetite and maghemite.* Two synthetic mixtures have been prepared as follows:

– sample MMAA:

11 mg of MMA0 + 4 mg of E9d

– sample MMAB:

11 mg of MMA0 + 4 mg of MM100

Sample E9d is a poorly crystallized maghemite (MCD ~ 18 nm) synthesized by a sol-gel method (da Costa *et al* 1994b). Sample MM100 is a well-crystallized commercial maghemite (Agfa). At room temperature the MS of both samples consist of one broad and asymmetric sextet, due to the almost complete overlap of the octahedral and tetrahedral patterns. Two asymmetric Lorentzian-shaped sextets were used, and the A-site center shift was constrained as $\delta_A = \delta_B - 0.12$ mm/s (da Costa *et al* 1994a). The hyperfine fields were found to be: $H_{hf,A} = 490$ kOe and $H_{hf,B} = 493$ kOe for sample E9d; and $H_{hf,A} = 500$ kOe and $H_{hf,B} = 501$ kOe for sample MM100.

The RT Mössbauer spectra of the mixtures are shown in Figures 4a and 4b. They closely resemble the spectra of the samples discussed in the preceding section, especially as far as the area ratios of the two patterns are

https://doi.org/10.1346/CCMN.1995.0430602 Published online by Cambridge University Press

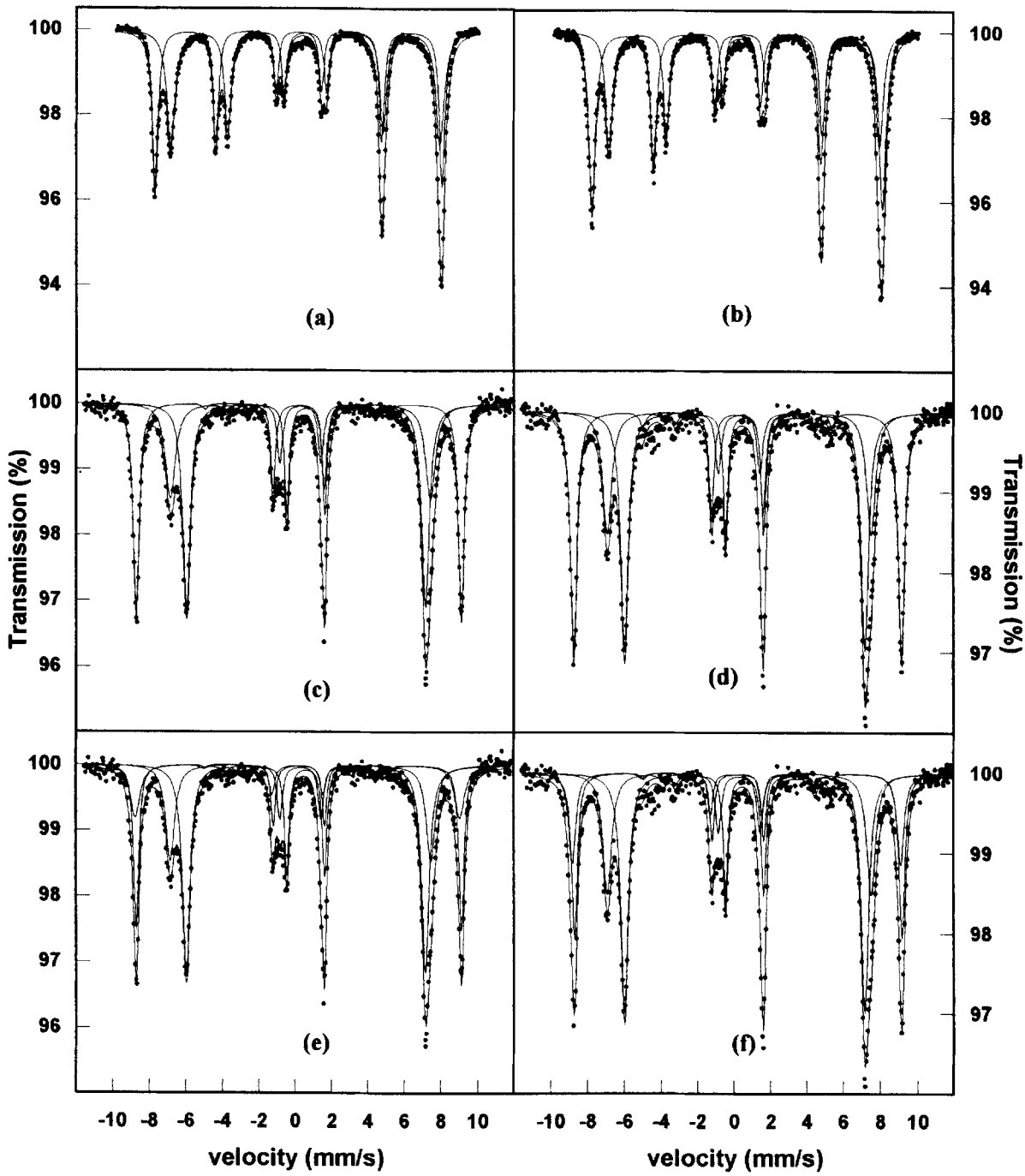


Figure 4. Mössbauer spectra of the synthetic mixtures: a) RT spectra of magnetite and poorly-crystallized maghemite (MMAA); b) RT spectra of magnetite and well-crystallized maghemite (MMAB). Applied-field (6T, 275 K) spectra: c) and e) refer to sample MMAA fitted with three and four sextets respectively; d) and f) refer to sample MMAB also fitted with three and four sextets respectively.

concerned. Both spectra could be adequately analyzed as a superposition of two Lorentzian sextets using the same restrictions as for sample MMA0, and the resulting parameters are given in Table 3. For the sake of simplicity we shall use the same site attribution as in pure magnetite, i.e., the high-field component will be called "A site" and the other "B site". Sample MMAB, which contains the well-crystallized maghem-

https://doi.org/10.1346/CCMN.1995.0430602 Published online by Cambridge University Press

Table 3. Mössbauer parameters at room temperature (upper part) and at 275 K under an applied field of 60 kOe (lower part) of synthetic mixtures of maghemite and magnetite. Estimated errors are: 1 kOe for the effective fields ($H_{eff}$), 4 kOe for the hyperfine fields ($H_{hf}$) and 0.01 mm/s for the isomer shifts ($\delta$).

| | $Fe_3O_4$ | | | | | | | | $\gamma$-$Fe_2O_3$ | | | | | | | |
|---|---|---|---|---|---|---|---|---|---|---|---|---|---|---|---|---|
| Sample | $H_{eff,A}$ (kOe) | $H_{hf,A}$ (kOe) | $\delta_A$ (mm/s) | RA (%) | $H_{eff,B}$ (kOe) | $H_{hf,B}$ (kOe) | $\delta_B$ (mm/s) | RA (%) | $H_{eff,B}$ (kOe) | $H_{hf,B}$ (kOe) | $\delta_B$ (mm/s) | RA (%) | $H_{eff,A}$ (kOe) | $H_{hf,A}$ (kOe) | $\delta_A$ (mm/s) | RA (%) |
| MMAA | — | 489 | 0.28 | 47 | — | 459 | 0.64 | 53 | — | — | — | — | — | — | — | — |
| MMAB | — | 492 | 0.28 | 59 | — | 458 | 0.66 | 41 | — | — | — | — | — | — | — | — |
| MMAA* | 553 | 493 | 0.30 | 33 | 407 | 467 | 0.69 | 41 | 443 | 503 | 0.39 | 26 | — | — | — | — |
| MMAB* | 555 | 495 | 0.29 | 36 | 408 | 468 | 0.69 | 40 | 448 | 508 | 0.39 | 24 | — | — | — | — |
| MMAA | 554 | 494 | 0.30 | 22 | 407 | 467 | 0.69 | 40 | 444 | 504 | 0.39 | 24 | 551 | 491 | 0.27 | 14 |
| MMAB | 553 | 493 | 0.30 | 22 | 408 | 468 | 0.69 | 40 | 448 | 508 | 0.39 | 24 | 559 | 499 | 0.27 | 14 |

* The last four numerical data do not correspond to the B-site of maghemite.

ite, has the "A-site" hyperfine field larger than sample MMAA. Furthermore, the relative area is also higher for this component: 59% in sample MMAB and 47% in MMAA. These results are easily understood considering that: i) the hyperfine fields of sample MM100 are larger than those in E9d; and ii) small-particle maghemite (E9d) usually has a broader hyperfine-field distribution, especially toward low-field values, and so it contributes more to the "B-site" absorption in the mixture.

The external-field spectra of both mixtures are shown in Figures 4c and 4d. Again, they are very similar to those obtained for sample MMA0 and MMAOH respectively. A three-sextets fit reproduces the experimental data in an acceptable manner, and the derived hyperfine parameters are included in Table 3. The relative area ratios of these three patterns are the same for both samples, as it would be expected since they contain the same amount of maghemite and magnetite. It is worth mentioning that the center shift for the extra component is again typical for $Fe^{3+}$ in an octahedral oxygen coordination. Although a three-sextet fit would seem to be acceptable as far as reproducing the spectra is concerned, it does not correspond to the physical reality since there are four distinct iron sites in the involved mixtures. This proves that even by applying a strong external field, it remains impossible to clearly separate the contribution of the A site of magnetite from that of maghemite. Attempts to fit four sextets with the same restrictions as mentioned in the previous section were successful (Figures 4e and 4f), and the various hyperfine parameters (Table 3) are all in good agreement with those of the composing compounds and with literature values for maghemite and magnetite.

*Nonstoichiometric magnetite.* Sample MAG00 is a supposedly pure large-particle magnetite which is part of the laboratory collection. Its cell parameter has been determined from the XRD reflections in the region 15–80° ($2\theta$) and it was found to be (0.8397 ± 0.0005) nm, in excellent agreement with literature values (JCPDS card # 19629). The particle size is in the same range as that for sample MM0, i.e., larger than 200 nm. The MS collected at RT is shown in Figure 5a, and its parameters derived from a two-sextet fit are listed in Table 4. The FWHM of lines 1 and 6 for the tetrahedral site ($\Gamma_A^{1,6}$) is 0.26 mm/s, whereas $\Gamma_B^{1,6}$ = 0.34 mm/s. This broadening of the B-site line has been discussed in detail by De Grave *et al* (1993). From the relative areas it is calculated that the occupation number is 1.9, very close to the theoretical value for stoichiometric magnetite.

Attempts to obtain nonstoichiometric magnetite were carried-out by heating sample MAG00 at selected temperatures and periods of time under a controlled partial pressure of oxygen. An example is sample MAG05, which was obtained after heating MAG00 at 1300°C during three hours in a atmosphere of $CO_2$ and then quenched in water. According to Dieckmann (1982) this procedure should produce nonstoichiometric magnetite. Heating for longer periods or at lower temperatures always produced hematite in addition to the spinel phase.

The XRD pattern in the region of 15–80° ($2\theta$, Co tube) of MAG05 shows exclusively the spinel reflections. The cell parameter was found to be (0.8393 ± 0.0005) nm, which is not significantly different from that of sample MAG00. This finding disagrees with that of Annersten and Hafner (1973) and of Randani *et al* (1987), who both observed a much smaller cell parameter for samples with approximately the same degree of nonstoichiometry as MAG05. This discrepancy will be discussed in detail later.

The MS recorded at RT for sample MAG05 is shown in Figure 5b. The hyperfine parameters as derived from a two-sextet fit, are the same as those of MAG00 (Table 4), but the occupation number has dropped to 1.3, suggesting a nonstoichiometric magnetite with approximate composition of $Fe_{2.94}O_4$. Both subpatterns are broadened as compared to MAG00: $\Gamma_A^{1,6}$ = 0.38 mm/s, and $\Gamma_B^{1,6}$ = 0.57 mm/s.

External-field measurements at 130 K were performed to obtain a more precise characterization of the

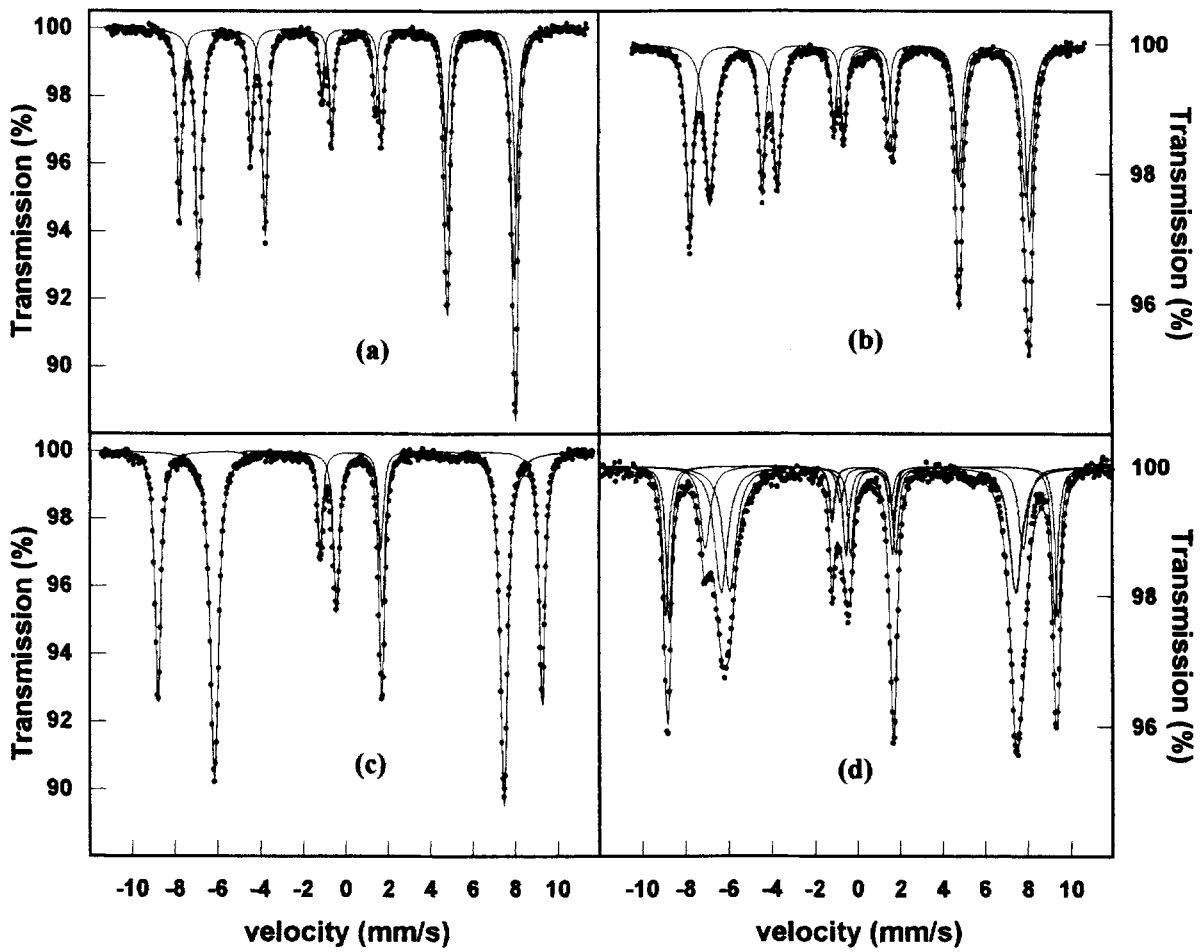


Figure 5. Room-temperature Mössbauer spectra of well-crystallized magnetite: a) original sample (MAG00), b) after annealing MAG00 at 1300°C in a controlled $O_2$ partial pressure (MAG05). Applied-field (6T, 130K) spectra: c) MAG00, d) MAG05 fitted as a mixture of magnetite and nonstoichiometric magnetite.

MAG00 and MAG05 samples. The spectrum of the first sample is depicted in Figure 5c. There is no indication that the middle lines are present and a two-quadruplet model accounts very well for the experimental data (full lines in Figure 5c). The derived parameters are listed in Table 4. The widths were found to be: $\Gamma_A^{1,6} = 0.33$ mm/s and $\Gamma_B^{1,6} = 0.41$ mm/s. This line broadening is known to occur on approaching the Verwey transition, and for a recent discussion on that subject the reader is referred to the work of De Grave *et al* (1993). The external-field spectrum of sample MAG05 shows the expected three-pattern structure, but two features, not observed in the MS for the aforementioned samples, have appeared: (i) the decoupled $Fe^{3+}$ pattern retains a considerable overlap with that of the presumed $Fe^{2.5+}$, and (ii) this latter component is extremely broad. The first trial fits using three Lorentzian-shaped quadruplets, yielded an unreasonably low value for the center shift of the octahedral ferric site. Moreover, the outer line width $\Gamma^{1,6}$ for the $Fe^{2.5+}$ component was found to be ≈0.8.mm/s, which is unacceptably broad for a sample presumed to be single phase. In a subsequent attempt, three model-independent distributions of hyperfine fields, accounting for any compositional disorder possibly existing in nonstoichiometric magnetite, have been considered. Apart from the difficulties to properly specify the intervals for the distinct distributions, it was consistently found that the center shift of the octahedral $Fe^{3+}$ component had a value close to 0.37 mm/s, which is much lower than commonly observed for spinel ferrites, and therefore believed to be unreal. Finally, a four-sextet fit, as applied to the MS of the mixed maghemite/magnetite samples described in the previous sections, would be meaningless since maghemite is unlikely to exist in MAG05 due to the high temperature used to prepare the sample.

At this point it is worth recalling that the X-ray

https://doi.org/10.1346/CCMN.1995.0430602 Published online by Cambridge University Press

Table 4. Hyperfine parameters of samples MAG00 and MAG05 at room temperature (upper part) and of sample MAG00 at 130 K in an applied field of 6T (lower part), assuming that $H_{ext}$ fully adds to $H_{hf,A}$ or subtracts from $H_{hf,B}$.

| Sample | $H_{hf,A}$ (kOe) | $\delta_A$ (mm/s) | $RA_A$ (%) | $H_{hf,B}$ (kOe) | $\delta_B$ (mm/s) | $RA_B$ (%) |
|---|---|---|---|---|---|---|
| MAG00 | 491 | 0.27 | 36 | 460 | 0.66 | 64 |
| MAG05 | 492 | 0.28 | 45 | 459 | 0.67 | 55 |
| MAG00 | 500 | 0.35 | 36 | 482 | 0.76 | 64 |

diffractogram of MAG05 presented no indication whatsoever for the presence of a phase other than a magnetite-like compound. Also, as argued above, a three-sextet fit, i.e., assuming single-phase, nonstoichiometric magnetite, cannot be accepted. Therefore, a next plausible possibility which requires further exploration is that MAG05 consists of a mixture of the type $(1\text{-}x)\ Fe_3O_4 + xFe_{3-v}O_4$, with v the average degree of nonstoichiometry. Since the sample has been prepared starting from a powder, it is not unlikely that v exhibits a more or less broad range of values. In that case, the MS is expected to be composed of a superposition of at least five subpatterns, namely two due to the magnetite and three due to the partly oxidized phase. It is obvious that several constraints had to be imposed in order for the iteration routine to reach convergency with reasonable adjusted parameter values. These constraints were: equal widths and center shifts for the two tetrahedral ferric components, equal widths for the two intermediate-valency states of octahedral iron, $\epsilon_Q = 0$ fixed for all quadruplets, and fixed B- to A-site area ratio of 2:1 for the magnetite subpattern (at low temperatures the ratio of the A- to B-site Mössbauer fractions in magnetite is close to 1). As shown in Figure 5d, this fitting procedure produced a reasonable reproduction of the observed line shape. However, as a result of the strong overlap of the various sub-components, and hence of the unprecise determination of the various Mössbauer parameters, only a few semi-quantitative conclusions can be derived from the model. These include that about half of the sample consists of the undisturbed magnetite phase, and that the average degree v of nonstoichiometry of the remaining half is situated within the range 0.1–0.2.

In summary, it has become clear from the present analyses that the zero-field MS (RT), reportedly to be characteristic for nonstoichiometric magnetite (Figure 5b), fail to provide a clear-cut characterization of the precise nature of the magnetite phase involved. Even the application of an external field with a strength of up to 6 T, seems to have its limitations in that respect. Obviously, more research work needs to be done on samples which have been prepared under proper, well-controlled conditions and which have been characterized by a range of various, complimentary techniques.

*X-ray diffraction results*

The diffractograms of all samples in the region from 15 to 80° ($2\theta$, Co tube) show the expected pattern of spinel structures, and no information about the samples' composition is apparent from them. Following the suggestion of Daniels and Rosencwaig (1969), a scan in the region of the (553) reflection can provide some indication about the presence of maghemite intermixed with magnetite. The step-scanned patterns of some selected samples are reproduced in Figure 6. Although an internal standard has not been used in these XRD measurements, it is believed that comparisons can be drawn between the results obtained for the various samples because exactly the same experimental conditions were applied for all of these measurements. In principle, the mixed sample MMAA is expected to exhibit two pairs ($K_{\alpha 1}$ and $K_{\alpha 2}$) of diffraction lines, one corresponding to magnetite and another one due to maghemite. The diffractogram in Figure 6a shows that the broad signal which can be attributed to the poorly crystalline maghemite phase is not readily distinguished from the sharper magnetite component. Its presence could only be confirmed after a numerical deconvolution procedure. The two unit-cell parameters and diffraction-line widths derived from this treatment are listed in Table 6. The former ones are reasonably close to those reported for magnetite and maghemite (JCPDS cards # 19.629 and 4.755) respectively. Daniels and Rosencwaig (1969) also scanned their samples in the region of the (210) and (213) reflections in order to reportedly demonstrate the absence of a maghemite impurity. However, these particular reflections are superstructure lines associated with a 1:5 ordered arrangement of the vacancies and iron species. Such ordering is unlikely to occur in small-particle maghemite (Haneda and Morrish 1977).

Samples MMA0N and MMA0H show similar XRD patterns (Figures 6b and 6c). It was found necessary to include two sets of pseudo-Lorentzian lines in order to describe the experimental data in an adequate way. The corresponding cell parameters are smaller for sample MMA0H, and this could imply a higher degree of oxidation (Table 5). Furthermore, the second component is much broader than the first one. It seems conceivable to propose that both samples are actually mixtures of magnetite, nonstoichiometric magnetites, and possibly maghemite as well. Samples MAG00 and MAG05 also exhibit patterns similar to the previous ones (Figures 6d and 6e), but due to their larger particle size the $K_{\alpha 1}$ and $K_{\alpha 2}$ reflections are better resolved. For sample MAG00, a broad, but weak contribution is observed to be superimposed to the background signal. Its origin has remained unclear. The main peak is very sharp and the cell parameter (0.8389 nm), calculated from its position, is smaller as compared to literature data quoted for magnetite, but similar to values ob-

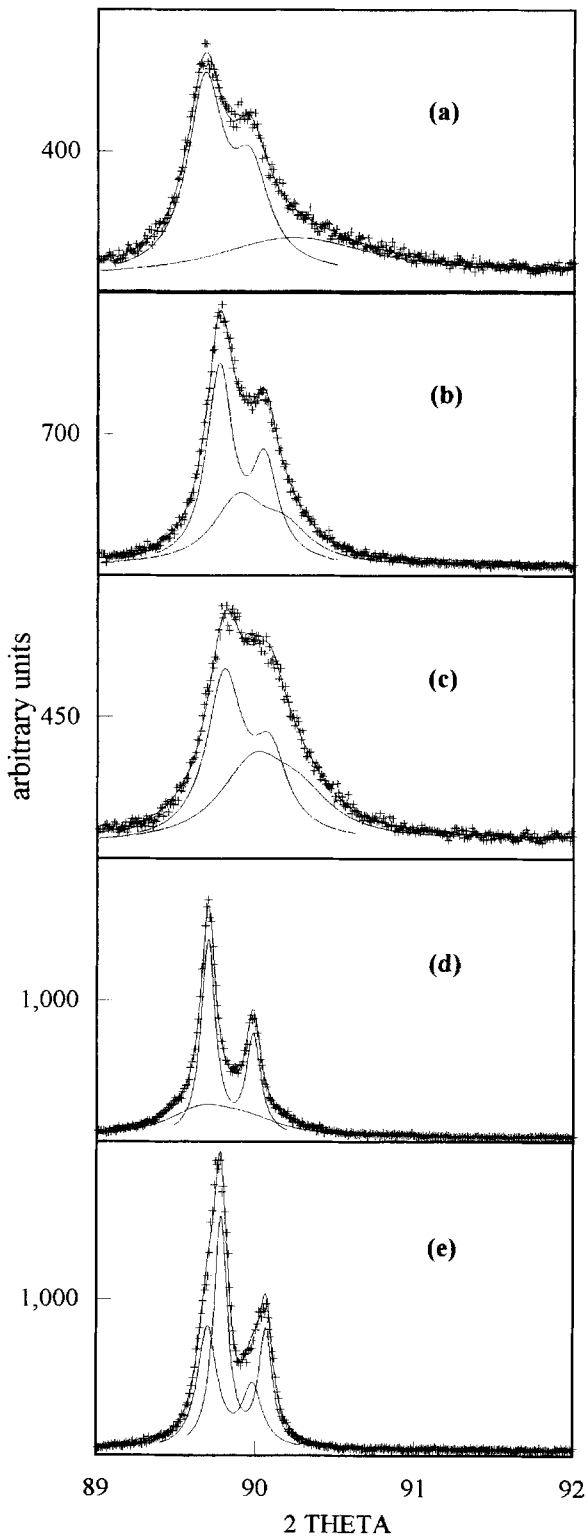


Figure 6. X-ray diffractograms (Cu K$\alpha$) in the region of the (553) reflection: a) synthetic mixture of magnetite and poorly crystallized maghemite (MMAA), b) small-particle magnetite one month after synthesis (MMA0N), c) small-particle magnetite heated at 80°C in air (MMA0H), d) large-particle magnetite (MAG00), e) previous sample annealed at 1300°C.

Table 5. X-ray diffraction parameters obtained from the step-scan from 89° to 92° (2$\theta$, Cu-tube) for some selected samples. Estimated errors for the cell parameters a1 and a2 are 0.0005 nm.

| Sample | a1 (nm) | FWHM (2$\theta$) | a2 (nm) | FWHM (2$\theta$) |
|---|---|---|---|---|
| MMAA | 0.8391 | 0.28 | 0.8356 | 1.1 |
| MMA0N | 0.8385 | 0.20 | 0.8376 | 0.39 |
| MMA0H | 0.8382 | 0.26 | 0.8369 | 0.48 |
| MAG00 | 0.8389 | 0.11 | — | — |
| MAG05 | 0.8389 | 0.15 | 0.8383 | 0.11 |

tained from reflections in the low-angle region. In contrast, the computer fit for sample MAG05 reveals two clearly distinct pairs of reflections, the less intense one ($\approx$40% of the total area) corresponding to a same unit-cell parameter as that found for sample MAG00. The second peak is shifted toward slightly higher diffraction angles, and is relatively sharp as well. In accordance with the high temperature at which this sample was prepared, no evidence for the presence of maghemite is inferred from the MAG05 diffractogram. In conclusion, the high-angle XRD scans seem to confirm that sample MAG05 is composed of magnetite and a non-stoichiometric magnetite phase. In contrast to samples MMA0 and MMA0H, the degree of nonstoichiometry appears to be well-defined, although it has remained impossible to determine its value from the present experiments. These XRD results are in qualitative agreement with those suggested by the Mössbauer analyses.

## CONCLUSIONS

The thermal decomposition products of large-particle magnetite have been identified as hematite and stoichiometric magnetite. On the other hand, the MS of the products obtained by heating small-particle magnetite could be successfully interpreted as the result of a simple mixture of magnetite and maghemite, instead of single-phase nonstoichiometric magnetite. This conclusion is found to be supported by the spectra of synthetic mixtures of magnetite and poorly- and well-crystallized maghemite. These latter spectra proved unequivocally that it is not feasible to resolve any contribution to the MS by the A-site ferric ions in magnetite from those in maghemite. Finally, it was shown that heating large-particle magnetite at 1300°C under a controlled atmosphere produced nonstoichiometric magnetite, however, with a non-unique degree of nonstoichiometry.

https://doi.org/10.1346/CCMN.1995.0430602 Published online by Cambridge University Press

## ACKNOWLEDGMENTS

This work was supported in part by the Fund for Joint Basic Research (Belgium, Grant nr. 2.0014.93) and by CNPq (Brazil).

## REFERENCES

Annersten, H., and S. S. Hafner. 1973. Vacancy distribution in synthetic spinels of the series $Fe_3O_4$-$\gamma$-$Fe_2O_3$. *Z. Kristallogr.* **137**: 321–340.

Aragon, R., D. J. Buttrey, J. P. Shepherd, and J. M. Honig. 1985. Influence of nonstoichiometry on the Verwey transition. *Phys. Rev. B* **31**: 430–436.

Armstrong, J. R., A. H. Morrish, and G. A. Sawatzky. 1966. Mössbauer study of ferric ions in tetrahedral and octahedral sites of a spinel. *Phys. Lett.* **23**: 414–416.

Bate, G. 1975. Oxides for magnetic recording. In *Magnetic Oxides, Vol. 2.* D. J. Craik, ed. London: John Wiley & Sons, 689–742.

Coey, J. M. D., A. H. Morrish, and G. A. Sawatzky. 1971. A Mössbauer study of conduction in magnetite. *J. Physique* **32**: C1-271–273.

da Costa, G. M., E. De Grave, L. H. Bowen, R. E. Vandenberghe, and P. M. A. de Bakker. 1994a. The center shift in Mössbauer spectra of maghemite and aluminum maghemites. *Clays & Clay Miner.* **42**: 628–633.

da Costa, G. M., E. De Grave, P. M. A. de Bakker, and R. E. Vandenberghe. 1994b. Synthesis and characterization of some iron oxides by sol-gel method. *J. Solid State Chem.* **113**: 405–412.

Daniels, J. M., and A. Rosencwaig. 1969. Mössbauer spectroscopy of stoichiometric and nonstoichiometric magnetite. *J. Phys. Chem. Solids* **30**: 1561–1571.

de Bakker P. M. A., E. De Grave, R. E. Vandenberghe, L. H. Bowen, R. J. Pollard, and R. M. Persoons. 1991. Mössbauer study of the thermal decomposition of lepidocrocite and characterization of the decomposition products. *Phys. Chem. Minerals* **18**: 131–143.

De Grave, E., R. M. Persoons, R. E. Vandenberghe, and P. M. A. de Bakker. 1993. Mössbauer study of the high-temperature phase of Co-substituted magnetites, $Co_x$-$Fe_{3-x}O_4$. I. $x \leq 0.04$. *Phys. Rev. B* **47**: 5881–5893.

Dieckmann R., and H. Schmalzried. 1977. Defects and cation diffusion in magnetite (I). *Ber. Bunsenges. Phys. Chem.* **81**: 344–347.

Dieckmann, R. 1982. Defects and cation diffusion in magnetite (IV): Nonstoichiometric and point defect structure of magnetite ($Fe_{3-\gamma}O4$). *Ber. Bunsenges. Phys. Chem.* **86**: 112–118.

Elder, T. 1965. Particle-size effect in oxidation of natural magnetite. *J. Appl. Phys.* **36**: 1012–1013.

Häggström, L., H. Annersten, T. Ericsson, K. W. Wäppling, and S. Bjarman. 1978. Magnetic dipolar and electric quadrupolar effects on the Mössbauer spectra of magnetite above the Verwey transition. *Hyperfine Interactions* **5**: 201–204.

Haley, G., J. G. Mullen, and J. M. Honig. 1989. First order change in hyperfine interaction at the Verwey transition in magnetite. *Solid State Comm.* **69**: 285–287.

Haneda, K., and A. H. Morrish. 1977. Vacancy ordering in $\gamma$-$Fe_2O_3$ small particles. *Solid State Comm.* **22**: 779–782.

Iida, S. 1980. Structure of $Fe_3O_4$ at low temperatures. *Phil. Mag.* **B42**: 349–376.

Kakol, Z., and J. M. Honig. 1989. The variation of Verwey transition temperature with oxygen stoichiometry in magnetite. *Solid State Comm.* **70**: 967–969.

Klug, H. P., and L. E. Alexander. 1974. *X-Ray Diffraction Procedures for Polycrystalline and Amorphous Materials.* New York: John Wiley and Sons.

Mørup, S., H. Topsøe, and J. Lipka. 1976. Modified theory for Mössbauer spectra of superparamagnetic particles: application to $Fe_3O_4$. *J. Physique* **37**: C6-287–290.

Mørup, S., and E. Tronc. 1994. Superparamagnetic relaxation of weakly interacting particles. *Phys. Rev. Lett.* **72**: 3278–3281.

Murad, E., and U. Schwertmann. 1993. Temporal stability of a fine-grained magnetite. *Clays & Clay Miner.* **41**: 111–113.

Randani, A., J. Steinmetz, C. Gleitzer, J. M. D. Coey, and J. M. Friedt. 1987. Perturbation de L'echange electronique rapide par les lacunes cationiques dans $Fe_{3-x}O_4$ ($x \leq 0.09$). *J. Phys. Chem. Solids* **48**: 217–228.

Sawatzky, G. A., F. Van der Woude, and A. H. Morrish. 1969. Recoilless-fraction ratios for $Fe^{57}$ in octahedral and tetrahedral sites of a spinel and a garnet. *Phys. Rev.* **183**: 383–386.

Steinthorsson, S., Ö. Helgason, M. B. Madsen, C. B. Koch, M. D. Bentzon, and S. Mørup. 1992. Maghemite in Icelandic basalts. *Mineral. Mag.* **56**: 185–199.

Sugimoto, T., and E. Matijevic. 1980. Formation of uniform spherical magnetite particles by crystallization from ferrous hydroxide gels. *J. Colloid Interface Sci.* **74**: 227–243.

Vandenberghe, R. E., and E. De Grave. 1989. Mössbauer effect studies of oxidic spinels. In *Mössbauer Spectroscopy Applied to Inorganic Chemistry, Vol. 3.* G. J. Long and F. Grandjean, eds. New York: Plenum, 59–182.

Verwey, E. J. W., and P. W. Haayman. 1941. Electronic conductivity and transition point of magnetite ($Fe_3O_4$). *Physica* **8**: 979–987.

*(Received 31 October 1994; accepted 13 March 1995; Ms. 2587)*